

Tribo-rheological behavior of the spherically contact with a UHMWPE viscoelastic plane

Haider Sh. Wahad

College of Food Science, Al- Qasim Green University, IRAQ

Abstract:

In this work the behavior of UHMWPE that used in knee prosthesis. The behavior of polyethylene at creep and friction due to indentation is analyzed. The behavior of polyethylene at relaxation situation under the action of the rigid indenter is deduced. determining the energy lost by hysteresis when indenting a surface flat of UHMWPE with a rigid conical indenter, and the spherical connection. Adopted the modified Zener rheological model are used, and the stress-strain curve of UHMWPE is approximated by Zener type models with different mechanical properties.

Key words: UHMWPE, knee prosthesis, Zener rheological model, creep, friction

1. Introduction

Knee replacement, also called **knee arthroplasty** or total **knee** replacement, is a surgical procedure to resurface a **knee** damaged by arthritis. Metal and plastic parts are used to cover the ends of the bones that form the **knee** joint, along with the kneecap. Phenomena that occur after total knee arthroplasty due to the friction process between UHMWPE polymer and metallic or ceramic materials. These phenomena are particularly complex and require interdisciplinary studies; they lead to the surface destruction of UHMWPE [1]. The friction process generates aspects of a micro-mechanical, physic-chemical, thermodynamic and irreversible nature, damage and destruction, in part or in all over of the polyethylene surface. For the contact of an indenter with known geometry (figure .1) with a viscoelastic plan from UHMWPE, the Zener viscoelastic behavior model is accepted, with some modifications. The change in the ideal Zener behavior due to the friction of polyethylene with the penetrator and the energy law of fluid.

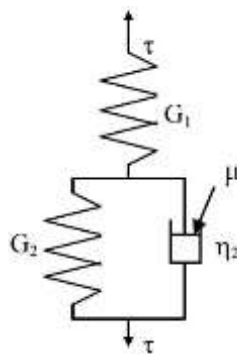


Figure .1 Modified Zener rheological model [2]

η_2 is the viscosity of UHMWPE polyethylene is considered, μ is the coefficient of friction of the UHMWPE polyethylene with the indenter, with conditions, the penetration of the rigid cone at a constant velocity involves the mechanical equilibrium equations:

$$\delta = \delta_1 + \delta_2 = k_{e_1} + k_{e_2} \cdot \left(F_n - \frac{A_c}{h_0} \cdot \eta_2 \cdot \delta_2 - \mu_2 \cdot F_n \right), \quad (1)$$

$$\dot{\delta} = \dot{\delta}_1 + \dot{\delta}_2 = k_{e_1} \cdot F_n + \dot{\delta}_2 \quad (2)$$

Where δ is the total load deformation under normal force F_n ; δ_1 , δ_2 are elastic and viscoelastic deformations; k_{e_1} , k_{e_2} are the polyethylene rigidities of the specimen (mm / N), dependent on the modules of elasticity (G_1 , G_2), and the geometry of the specimen, experimentally determinable. A_c is the contact area between the surface / specimen and the indenter, related to the thickness of the surface / specimen.

$\dot{\delta}$, $\dot{\delta}_1$, $\dot{\delta}_2$ are Partial derivatives of indentation with respect to time, From eq.(1) and eq.(2) the differential equation behavior of the UHMWPE corresponding to the contact with the indenter rigid cone - spherical connection is deduced.

$$\delta + A_c \cdot \eta_2 \cdot k_{e_1} \cdot \dot{\delta} = (k_{e_1} + k_{e_2} - \mu_2 \cdot k_{e_2}) \cdot F_n + k_{e_1} \cdot k_{e_2} \cdot A_c \cdot \eta_2 \cdot \dot{F}_n \quad (3)$$

This differential equation can be solved with the following conditions: (a) loading at constant deformation velocity ($\delta \neq v_0$) and time force dependence is obtained; (b) loading at constant force F_0 , resulting the dependence of the deformation on the applied force. The behavior of UHMWPE polyethylene at frictional indentation is analyzed based on equation (3), accepting loading at constant velocity ($h = v_0, \dot{h} = v_0 \cdot t$). Under these conditions, the solution of the linear differential equation (3) becomes:

$$F_n = \frac{B - AC}{A^2} \cdot e^{-At} + \frac{B}{A} \cdot \left(t - \frac{1}{A}\right) + \frac{C}{A}, \quad (4)$$

where A, B, C are the material-specific parameters and loading conditions:

$$A = \frac{k_{e1} + k_{e2} - \mu_2 \cdot k_{e2}}{k_{e1} \cdot k_{e2} \cdot A_c \cdot \eta}; \quad B = \frac{v_0}{k_{e1} \cdot k_{e2} \cdot A_c \cdot \eta}; \quad C = \frac{v_0}{k_{e1}}. \quad (4.a)$$

Behavior of polyethylene at creep due to indentation is analyzed based on equation (3), considering the constant load $F_n = F_{n0}$ ($F_n = 0$); the differential equation is obtained of the linear type. Integrating, with boundary conditions, $\delta = \delta_0$; $t = 0$ is :

$$\delta(t) = \left(\delta_0 - \frac{A_1}{B_1} \cdot F_{n0}\right) \cdot e^{-A_1 t} + \frac{B_1}{A_1} \cdot F_{n0}, \quad (5)$$

where A_1, B_1 are specific parameters having the expressions:

$$A_1 = \frac{1}{k_{e2} \cdot A_c \cdot \eta}; \quad B_1 = \frac{k_{e1} + k_{e2} - \mu_2 \cdot k_{e2}}{k_{e2} \cdot A_c \cdot \eta}. \quad (5.a)$$

The creep function of polyethylene $\Phi(t)$ under the rigid indenter is defined as the response of the material to the constant load, as follows:

$$\Phi(t) = \frac{\delta(t)}{F_{n0}} = \left(k_{e1} - \frac{B_1}{A_1}\right) \cdot e^{-A_1 t} + \frac{A_1}{B_1}. \quad (6)$$

At the initial moment, the instantaneous deformation becomes:

$$\delta_0 = k_{e1} \cdot F_{n0}.$$

The behavior of polyethylene at relaxation situation under the action of the rigid indenter is deduced from equation (3), considering the constant deformation $\delta = \delta_0$, ($\dot{\delta} = 0$). By integration, under the boundary conditions: $F_n = F_{n0}$ for $t = 0$, we obtain:

$$F_n(t) = \left(F_{n0} - \frac{B_2 \cdot \delta_0}{A}\right) \cdot e^{-At} + \frac{B_2 \cdot \delta_0}{A}, \quad (7)$$

with relation A (relation 4.a) and

$$B_2 = \frac{1}{k_{e1} \cdot k_{e2} \cdot A_c \cdot \eta} \quad (8)$$

The relaxation function of polyethylene, $\Psi(t)$, under the rigid indenter is defined as the response of the material to constant deformation, as follows:

$$\Psi(t) = \frac{F_n}{\delta_0} = \left(\frac{1}{k_{e1}} - \frac{B_2}{A}\right) \cdot e^{-At} + \frac{B_2}{A}. \quad (9)$$

2. The effect of energy surface on the coefficient of friction

Friction patterns described the effects on polyethylene according to a law of flow similar to that of metals [3], [4]. This type of modeling is not suitable for UHMWPE, due to the fundamental differences in the deformation mechanisms of polymers and metals. A model is adopted in which the state variables evolve according to the deformation speed. The energy lost in the process of damage to polyethylene will be used as an indicator of wear [1].

The aim of this study was to determine the energy lost by hysteresis when indenting a flat UHMWPE surface with a rigid conical indenter, and spherical connection.

Indentation is defined as the process of penetration of the surface to be studied by a penetrator called "indenter" (with various geometric shapes), which penetrates the surface to a certain depth due to the action of a force of controlled magnitude and direction followed by its withdrawal. UHMWPE is a polymer with viscoelastic behavior; in fact, UHMWPE is considered as an elastovascular body, which deforms elastically, the deformations occur that lead to flow (as to a fluid body) [5]. The viscoelastic behavior interprets the variation of the deformation under the action of constant stress(applied stress) for a period of time. The deformation initially shows an elastic response, at applied stress, and a delayed elastic deformation. In the present study, adopted the modified Zener rheological model Figure 4.1, composed of a spring inserted with a Voigt-Kelvin element [6], (a spring connected in parallel with a damper) of high molecular weight polyethylene, UHMWPE. The stress-strain curve of UHMWPE is approximated by Zener type models with different mechanical properties. Consider the external coefficient of friction and the fluid friction law:

$$\tau_f = \eta_2 \cdot \dot{\varepsilon}_0 \cdot \left(\frac{\dot{\delta}}{\dot{\delta}_0} \right)^{m_e} \quad (10)$$

The force in the Damper is defined as:

$$F_{nv} = A \cdot \tau_f + \mu \cdot F_n = A \cdot \eta_e \cdot \dot{\varepsilon}_0 \cdot \left(\frac{v}{v_0} \right)^{m_e}, \quad (11)$$

Where $\varepsilon_0 \equiv \frac{1}{s}$, $v_0 = \delta_0 = 1 \text{ mm}$, are constants of consistency

η_e is the equivalent viscosity of UHMWPE, global friction parameter (internal or external). For ease of calculation the creep functions Φ_{am} and relaxation function Ψ_{am} , are dimensionless to time, and described as a condition for connecting the Zener deformation with normal load, by the following relations:

$$\Phi_{am} = \Phi_m \cdot G_2 = \frac{1}{g_{12}} + (1 - \exp(-t_a)), \quad (12a)$$

$$\Psi_{am} = \frac{\Psi_m}{G_2} = \frac{g_{12}}{1 + g_{12}} \cdot [1 + g_{12} \cdot \exp(-t_a \cdot (1 + g_{12}))]; \quad (12b)$$

Where t_a is dimensionless time, $t_a = \frac{t}{t_i}$, t_i is the delay time, $t_i = \frac{\eta_2}{G_2}$; g_{12} is elasticity parameter $g_{12} = \frac{G_1}{G_2}$, dimensionless functions of Creep and relaxation, Φ_{am} , and Ψ_{am} , (Figure. 2) shows continuous variations (relative to the dimensionless time, t_a , and the elasticity parameter, g_{12}).

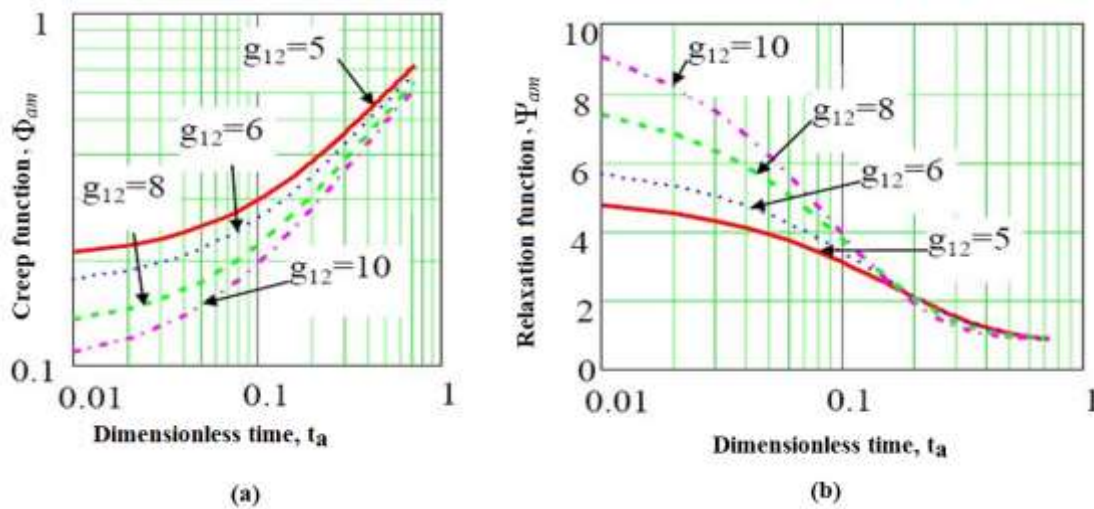


Figure. 2 dimensionless functions of creep a) and relaxation b) of a modified Zener viscoelastic material

The variation of the contact area and the pressure distribution is analyzed for different loading or unloading conditions. It can be considered as an initial solution that the stresses and strains corresponding to a purely elastic material are known (V. Radok-Johnson [6]).

This involves the replacement of the elastic constant in the elastic solution by the integral operator from the viscoelastic stress-strain relations. If the deformation beginning is known, the stresses are found by replacing the elastic modulus, $2G$, in the elastic solution by the integral operator, expressed in terms of the relaxation function. If the load is known, the variation in deformation is found in the elastic solution by replacing the $1 / 2G$ constant with the integral operator involving the creep compliance function $\Phi_m(t)$.

3. Indentation model with rigid cylindrical indenter

The contact between a rigid penetrator with a cylindrical tip and a viscoelastic plane is analyzed. The geometry of this penetrator is presented in Figure.3

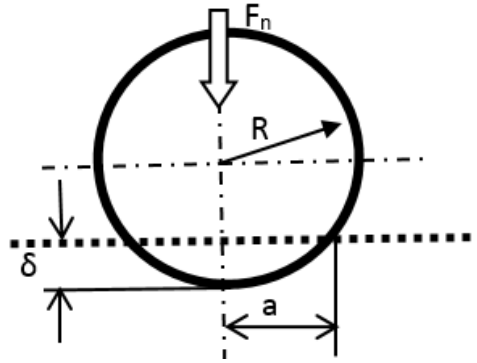


Figure.3 Rigid cylindrical penetrator geometry.

Indentation is defined by the following geometric parameters:

α - conic taper;

R - radius of the connecting sphere at the top of the cone;

δ - maximum penetration depth (indentation);

a - radius of the contact circle;

δ_s - penetration depth (indentation) corresponding to the limit of the spherical area;

a_s - the radius of the contact circle corresponding to the boundary of the spherical area;

h_0 - height of the cone.

For calculation, the penetration depth and the radius of the contact circle are dimensionless to the radius of the sphere at the tip of the cylinder R, : $\delta_a = \frac{\delta}{R}$, $a_a = \frac{a}{R}$. The loading of the cylinder is estimated by the average pressure Striebeck.

$$p_s = \frac{F_n}{B \cdot 2 \cdot R}; p_{as} = \frac{p_s}{G_2} \quad (13)$$

dimensionless half-width contact of the indenter is:

$$a_a(t_a, g_{12}, F_{as}) = \left\{ \frac{4}{\pi} \cdot F_{as} \cdot \left[\frac{1}{g_{12}} + \frac{1}{1} \cdot (1 - \exp(-t_a)) \right] \right\}^{\frac{1}{2}} \quad (14)$$

At the initial moment ($t_a = 0$), the contact half-width is:

$$a_{ao}(F_{as}, g_{12}) = \left(\frac{4}{\pi \cdot g_{12}} \cdot F_{as} \right)^{\frac{1}{2}}$$

For a known indentation speed (v), the dimensionless indentation depth is

$$\delta_a = \frac{\delta}{R} = v_a \cdot t_a \quad (15)$$

where the dimensionless velocity is defined as $v_a = (\eta e \cdot v) / (G_2 \cdot R)$ and t_{oa}

is the dimensionless time corresponding to the maximum load force.

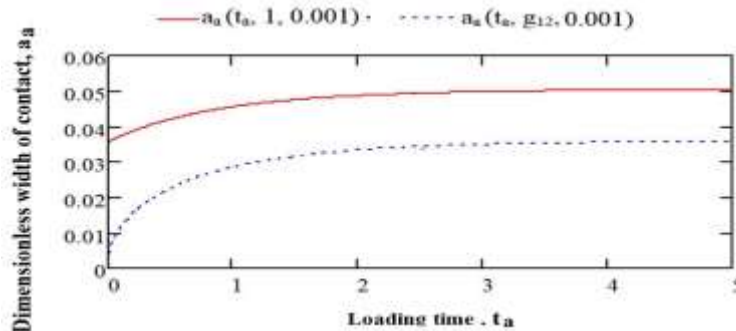


Figure 4. Dimensionless contact half-width variation with loading time

The response of the material to creep is

$$s(t_s) = \int_0^{t_a} \Psi(t_a - x) \cdot \frac{da_a^2}{d\delta_a} dx \quad (16)$$

If the variation of the dimensionless penetration depth $\delta_a(t)$ is known, then the variation of the dimensionless contact radius $a_a(t)$ is given by the equation:

$$a_a(t) = \sqrt{\delta_a(t)} \quad (17)$$

It can be substituted in equation (4.16) to find the dimensionless contact pressure Striebeck:

$$p_{as} = 4 \cdot \int_0^{t_a} \Psi(t_a - x, g_{12}) \cdot \left[\frac{d}{dx} \left[a_{ao}(x, F_{as}, g_{12}) \cdot (1 - r_a^2)^{\frac{1}{2}} \right] \right] \quad (18)$$

At some point, the pressure in the center of the linear contact is

$$p_{ot} = \frac{2}{\pi} \cdot \frac{F_n}{a(t)} \quad (19)$$

the relative pressure $p_{otr} = \frac{p_{ot}}{p_{oo}}$, p_{oo} is the pressure in the linear center of contact at time $t = 0$, the variation of the pressure on the contact belt of the rigid cylinder with polyethylene considered as material with Zener behavior is deduced:

$$p_r(r_a, t_a, g_{12}) = p_{otr}(t_a, g_{12}) \cdot \sqrt{1 - \frac{r_a^2}{[1 + g_{12} \cdot (1 - \exp(-t_a))]^2}} \quad (20)$$

Thus, Figure 5 exemplifies the variation of the dimensionless pressure at different points on the section of contact ($r_a = 0; 0.5; 0.8; 1; 1.2; 1.5$) with the dimensionless time, for the Viscoelasticity parameter, $g_{12} = 84.12$.

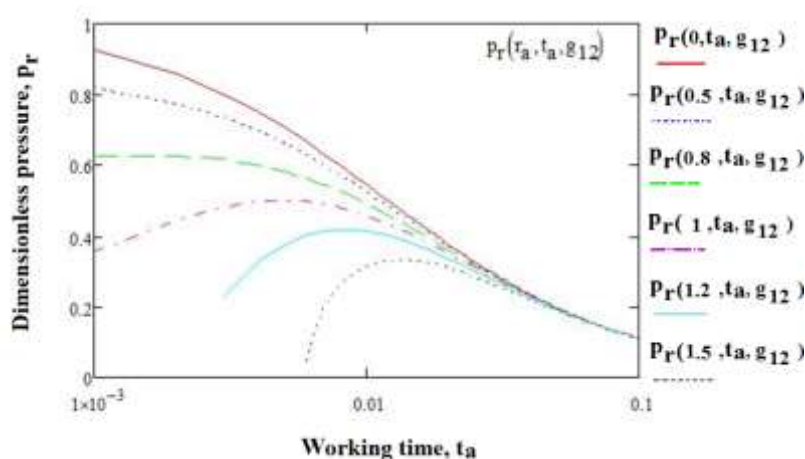


Figure.5 variation of the dimensionless pressure between the cylinder and the viscoelastic plane with the working time
When the rheological properties of polyethylene change, especially as a result of temperature, the pressure distribution is as shown in Figure .6.

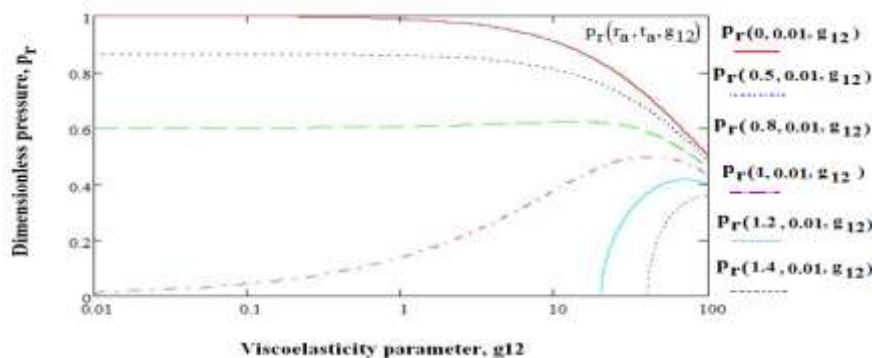


Figure.6 variation of the dimensionless pressure between the cylinder and the plane with variable Viscoelasticity

When the external load is variable, a real situation in the knee prosthesis, a linear variation between the minimum force (F_{am}) and the maximum force (F_{aMS}) is accepted. In this case, the contact width has the expression

$$a_{alin}(t_a, g_{12}, F_{aMS}, F_{am}, t_{a1}, t_{a2}) = \left[\frac{4}{\pi} \cdot F_{aSM} \cdot \int_0^{t_a} \Phi_{am}[(t_a - x), g_{12}] \frac{d}{dx} F_a(F_{am}, t_{a1}, t_{a2}, x) dx \right]^{\frac{1}{2}} \quad (21)$$

The variation of the contact (half-width) with time and with the load, allows the theoretical analysis of the component of losses by the coefficient of friction hysteresis (μ_h). Thus, for cylindrical contact, this component has the form [7]:

$$\mu_h = 2 \cdot \left(\frac{4}{\pi}\right)^3 \cdot \alpha_h \cdot \frac{B}{2 \cdot R} \cdot \left(\frac{p_m}{E_s}\right)^4 \quad (22)$$

where p_m is the average contact pressure, time-dependent and viscoelastic properties of polyethylene, E_s - equivalent elasticity, α_h - loss coefficient by hysteresis. The equation (22) has the expression

$$\mu_h(t_a, g_{12}, F_{aS}, B_a, \alpha_h) = 2 \cdot \left(\frac{4}{\pi}\right)^3 \cdot \alpha_h \cdot B_a \cdot \left(\frac{1 + g_{12}^{-1}}{3} \cdot \frac{F_{aS}}{a_a(t_a, g_{12}, F_{aS})}\right)^4 \quad (23)$$

Figure .7 and Figure .8 exemplify the variation of the Coefficient of hysteresis friction, with time and with the viscoelastic parameter, g_{12} respectively.

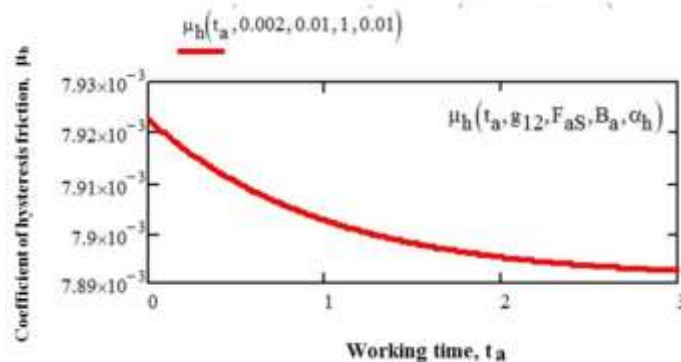


Figure. 7. Variation of the coefficient of friction with the working time

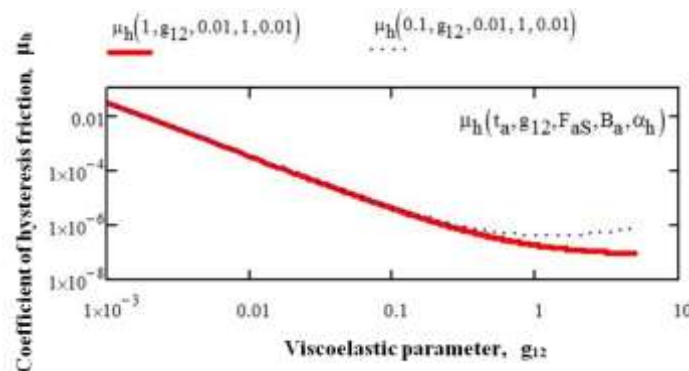


Figure. 8. Variation of the coefficient of friction with the viscoelastic parameter

4. Viscoelastic behavior of UHMWPE polyethylene in cylindrical contacts

It is known that UHMWPE polyethylene has a viscoelastic behavior, in which the intrinsic properties of elasticity and viscosity are manifested simultaneously. In order to analyze the behavior of UHMWPE polyethylene in the total knee prosthesis, it is assumed to detail the behavior for cylindrical contacts. The case of a rigid cylinder moving with sliding, rolling or sliding and rolling on a viscoelastic plane is accepted. The cylinder moves at a constant speed v (see Figure. 9) much slower than the speed of propagation of sound waves (v_s) in the viscoelastic body. In this hypothesis the inertial effects of the equilibrium equations can be neglected [8], [9]. The propagation speed of sound waves is $v_s \approx 5 \cdot 10^3$ m / s for steel, $v_s \approx 1000$ m / s for polymeric materials, $v_s \approx 30-50$ m / s for rubber. The solution given by Goryacheva and some adaptations by Popov [9] and Johnson [6] are accepted. The plastic properties of polyethylene are the longitudinal modulus of elasticity (E) and the Poisson's ratio (ν). The properties that characterize the viscous behavior of polyethylene are the characteristic creep (T_ϵ) and relaxation (T_σ) times. For the isotropic viscoelastic solid, the relationships between stresses and deformation have the forms

$$\epsilon_{x_0} + T_\epsilon \cdot \frac{\partial \epsilon_{x_0}}{\partial t} = \frac{1-\nu^2}{E} \cdot \left(\sigma_{x_0} + T_\sigma \cdot \frac{\partial \sigma_{x_0}}{\partial t} \right) - \frac{\nu \cdot (1+\nu)}{E} \cdot \left(\sigma_{z_0} + T_\sigma \cdot \frac{\partial \sigma_{z_0}}{\partial t} \right) \quad (34)$$

$$\begin{aligned} \varepsilon_{z_0} + T_\varepsilon \cdot \frac{\partial \varepsilon_{z_0}}{\partial t} &= \frac{1-\vartheta^2}{E} \cdot \left(\sigma_{z_0} + T_\sigma \cdot \frac{\partial \sigma_{z_0}}{\partial t} \right) - \frac{\vartheta \cdot (1+\vartheta)}{E} \cdot \left(\sigma_{x_0} + T_\sigma \cdot \frac{\partial \sigma_{x_0}}{\partial t} \right) \\ \gamma_{x_0 z_0} + T_\varepsilon \cdot \frac{\partial \gamma_{x_0 z_0}}{\partial t} &= \frac{1+\vartheta}{E} \cdot \left(\tau_{x_0 z_0} + T_\sigma \cdot \frac{\partial \tau_{x_0 z_0}}{\partial t} \right) \end{aligned}$$

Where $\varepsilon_{x_0}, \varepsilon_{z_0}, \gamma_{x_0 z_0}$ are deformation at the points (x_0, z_0) , and $\sigma_{x_0}, \sigma_{z_0}, \tau_{x_0 z_0}$ are the stresses at the points (x_0, z_0) . At any point (x, z) is defined by the velocity v and the time t :

$$z = z_0, x = x_0 - v \cdot t \quad (35)$$

Displacements and stresses are independent of time,

$$w_0(x + v \cdot t, t) = w(x), u_0(x + v \cdot t, t) = u(x)$$

The instantaneous modulus of elasticity is defined: $H = \frac{T_\varepsilon E}{T_\sigma}$, with $T_\varepsilon > T_\sigma$, parameter $\frac{T_\varepsilon}{T_\sigma} \approx 10^5 - 10^7$, for amorphous polymeric materials, $\frac{T_\varepsilon}{T_\sigma} \approx 10 - 10^2$ for polymeric materials with a high level of crystallinity, and $\frac{T_\varepsilon}{T_\sigma} \approx 1.1 - 1.5$ for dark colored materials.

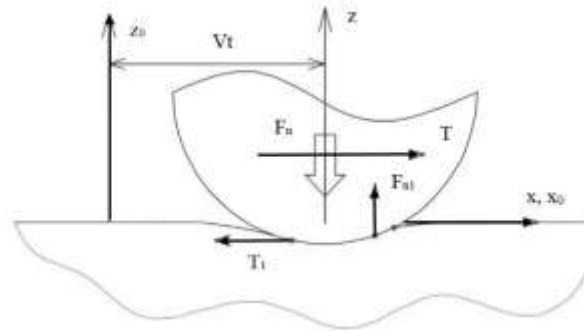


Figure. 9. Scheme of displacement on the plane

In the case of small deformations, the equation of the profile of the radius R of circular cylinder, can be approximated with a parabola

$$f(z) = \frac{z^2}{2 \cdot R} \quad (36)$$

the boundary condition of the undeformed surface ($z = 0$), The normal displacement in the $z, (w)$ direction of the half-space ($z = 0$), $w = f(z) + \text{const}$, inside the contact area $(-a, b)$ satisfies the condition

$$(z=0) \cdot \frac{\partial w}{\partial z} = \frac{z}{R} \quad (37)$$

It is accepted with the surface of contact that the tangential stresses τ_{xz} comply with Coulomb's law

$$(z=0) \tau_{xz} = -\mu \cdot \sigma_z \cdot \text{sign}(v) \quad (38)$$

where μ is the sliding friction coefficient. The stresses and displacements were described by Goryacheva, by solving the differential equations (34). Thus, the pressure $p(x)$ at any point in the contact area has the expression

$$\begin{aligned} p_x = -\sigma_z(x, 0) &= -\frac{\rho \exp(x/T_\sigma v)}{T_\sigma \cdot v \cdot \pi \cdot K \cdot R} \cdot \int_{-a}^x \left[\frac{(a+b)^2}{2} \cdot \left(\frac{1}{4} - \eta^2 \right) + F_n \cdot K \cdot R + (x' - T_\varepsilon \cdot v) \cdot \right. \\ &\left. (a+b) \cdot \left(\frac{1}{2} - \eta \right) - (x' - T_\varepsilon \cdot v) \cdot (a+x') \right] \cdot \frac{\exp\left(-\frac{x'}{T_\sigma v}\right) dx'}{(a+x')^{1/2+\eta} \cdot (b-x')^{1/2-\eta}} \end{aligned} \quad (39)$$

where $K = \frac{2 \cdot (1-\vartheta^2)}{\pi \cdot E}$; $\theta = \frac{1-2 \cdot \vartheta}{2 \cdot (1-\vartheta)}$; $\rho = \frac{1}{\sqrt{1+\mu^2 \cdot \theta^2}}$; $\eta = \frac{1}{\pi} \cdot \arctg(\mu \cdot \theta) \text{sign}(v)$, $|\eta| < \frac{1}{2}$;

and F_n is the normal force per unit length of the cylinder

$$F_n = \int_{-a}^b p(x) dx \quad (40)$$

$L = a + b$, the contact width of the rigid cylinder with the viscoelastic plane, $L_E = \sqrt{\frac{2 \cdot F_n \cdot K \cdot R}{\left(\frac{1}{4} - \eta^2\right)}}$

the contact width of the rigid cylinder on the elastic plane, $\alpha = \frac{T_\varepsilon}{T_\sigma}$, and $\zeta = \frac{L}{2 \cdot T_\varepsilon \cdot v}$

deduces the dimensionless contact width[8] $L_a = L/L_E$,

$$\left[1 - L_a^2 \right] \cdot \left[\Psi\left(\frac{3}{2} + \eta, 3; 2\zeta\right) \cdot \Phi\left(\frac{1}{2} + \eta, 1; 2\alpha\zeta\right) + \frac{1}{2} \cdot \alpha \cdot \left(\frac{1}{2} - \eta\right) \cdot \Psi\left(\frac{1}{2} + \eta, 1; 2\zeta\right) \right] \cdot (41)$$

$$\Phi\left(\frac{3}{2} + \eta, 3; 2\alpha\zeta\right)] + L_a^2 \cdot (1 - \alpha) \cdot \Psi\left(\frac{3}{2} + \eta, 3; 2\zeta\right) \cdot \Phi\left(\frac{3}{2} + \eta, 3; 2\alpha\zeta\right) = 0$$

where the hypergeometric confluent functions $\Psi(\beta, \gamma; z)$ and $\Phi(\beta, \gamma; z)$ have the parameters β and γ and the argument z :

$$\Psi(\beta, \gamma; z) = \frac{1}{\Gamma(\beta)} \cdot \int_0^\infty \exp(-zt) \cdot t^{\beta-1} \cdot (1+t)^{\gamma-\beta-1} \cdot dt$$

$$\Phi(\beta, \gamma; z) = \frac{1}{B(\beta, \gamma - \beta)} \cdot z^{1-\gamma} \cdot \int_0^z \exp(t) \cdot t^{\beta-1} \cdot (z-t)^{\gamma-\beta-1} \cdot dt$$

where $\Gamma(\beta)$ is the Gamma function, $\Gamma(\beta) = \int_0^\infty x^{\beta-1} \cdot e^{-x} dx$, $B(\beta, \gamma)$ is the Beta function, Figure .10 exemplifies the dimensionless contact width (L_a) with the variation of the rolling velocity of the rigid cylinder on UHMWPE polyethylene.

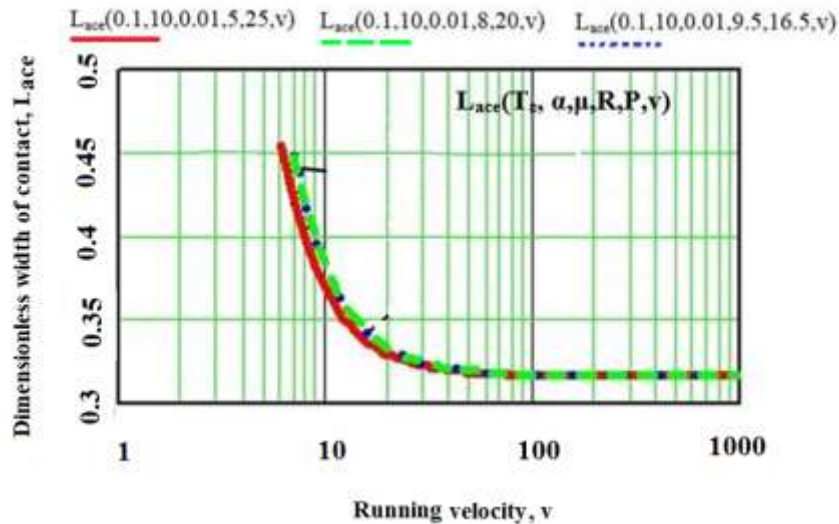


Figure 10. Variation of the dimensional contact width with rolling velocity

The coordinates of the points that define the contact width of the viscoelastic material can be found:

$$\begin{cases} L = a + b \\ \varepsilon = \frac{b - a}{b + a} \end{cases} \quad (42)$$

$$\text{with } \varepsilon = -2 \cdot \eta + \frac{(1-L_a^2) \cdot \left(\frac{1}{2} - \eta\right) \cdot \Psi\left(\frac{1}{2} + \eta, 1; 2\zeta\right)}{2 \cdot \zeta \cdot L_a^2 \cdot \Psi\left(\frac{3}{2} + \eta, 3; 2\zeta\right)} \quad (43)$$

Where $a_a = \frac{a}{L}$, $b_a = \frac{b}{L}$, it results from (42)

$$a_a = \frac{1-\varepsilon}{2} \text{ and } b_a = \frac{1+\varepsilon}{2}. \quad (44)$$

Figure 11 exemplifies the coordinates of the contact points as a function of speed for two rigid cylinders with radii $R = 5$ and $R = 9.5$.

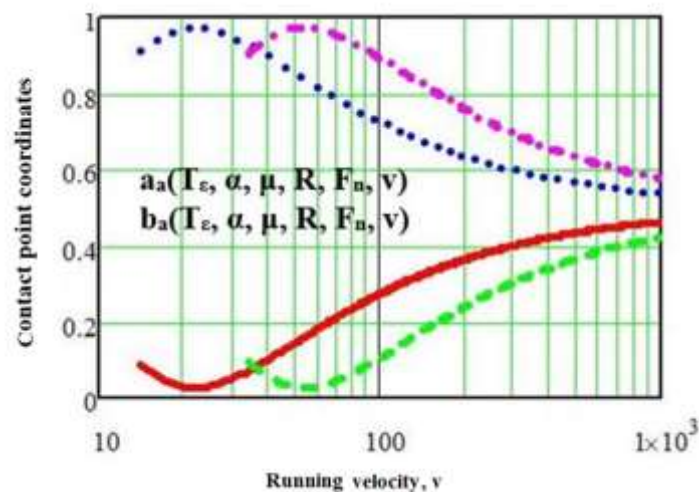


Figure .11 Coordinates of contact point depending on velocity

Due to the asymmetry of the pressure distribution ($a \neq b$), the reaction F_n , of the viscoelastic half-plane does not pass through the center of the cylinder. Thus, a torque (rolling moment) results.

$$.M_1 = \int_{-a}^b x \cdot p(x)xd \tag{45}$$

Replacing pressure $p(x)$ from eq.(39) to eq. (45) and the dimensionless rolling moment is M_1 , $M_{1a} = M_1 / (F_n \cdot L)$, results :

$$.M_{1a} = L_a^2 \cdot \left(\frac{1}{2\zeta} - \frac{\varepsilon}{2} - \frac{\eta}{3} \right) + \left(\frac{\varepsilon}{2} - \frac{1}{2\zeta\alpha} - \eta \right) \tag{46}$$

The tangential force $T_1 = \mu \cdot F_n$ is applied at the coordinate point $(0, d)$ and as a result the torque $M_2 = \mu \cdot F_n \cdot d$, according to the law of action and reaction $M_1 = M_2$, d is the distance from the axis of rotation to the position of the force is applied.

$$.d = \frac{M_1}{\mu \cdot F_n} = \frac{M_{1a} \cdot F_n \cdot L}{\mu} \tag{47}$$

$$\text{Or } d_a = \frac{d}{R} = \frac{M_{1a} \cdot L}{\mu \cdot R} \tag{48}$$

Figure .12 and Figure .13 exemplify the dimensionless rolling moment in eq.(46) and the dimensionless tangential force in eq.(48) as a function of the velocity v , for different radii of the cylinder (R).

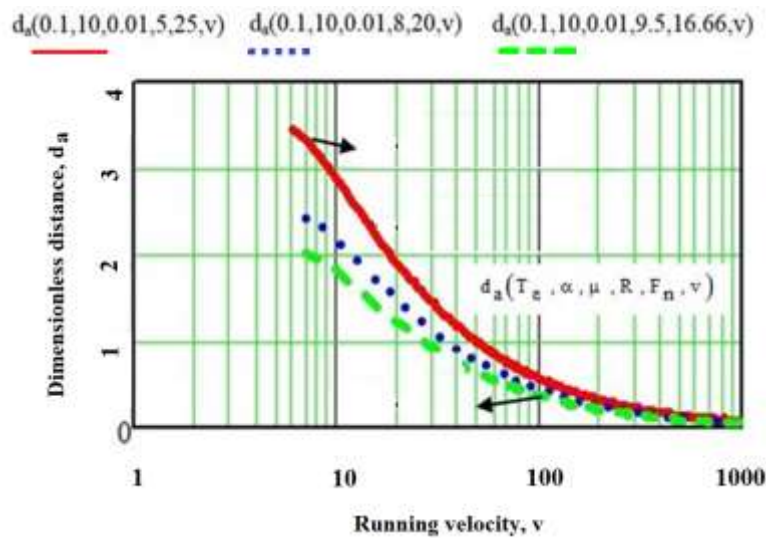


Figure .12. Dimensionless distance as a function of rolling velocity

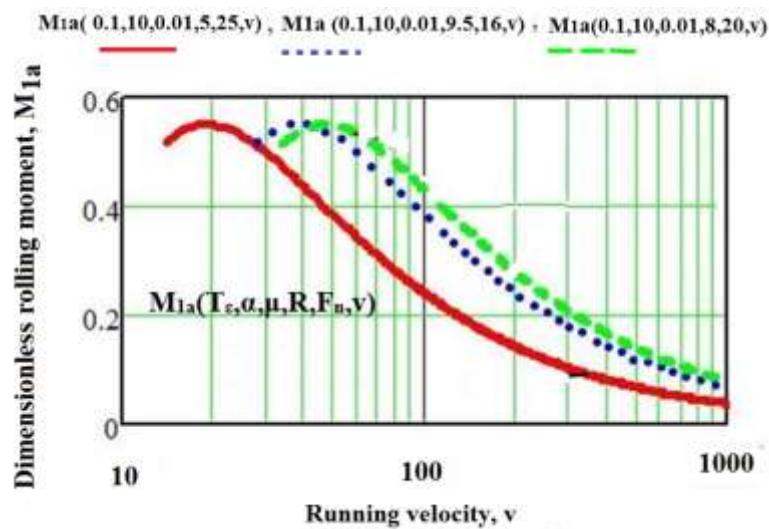


Figure .13. Dimensionless rolling moment as a function of running speed

To determine the coefficient of friction by rolling, it is considered that in the contact area $(-a, b)$ there are two parts: one with slip $(-a, c)$ and one with adhesion (stick) (c, b) . Figure.14 shows the scheme of contact with sliding and rolling. Assuming the rigid cylinder and the flat support made of polyethylene as a viscoelastic material, the tangential velocities of the contact points in the stick area (c, b) are:

$$.V - \omega R = \frac{\partial w_2^o}{\partial t} \tag{49}$$

where w_2^o is the displacement of the plane 2 with respect to the fixed system of axes x_0Oz_0 .

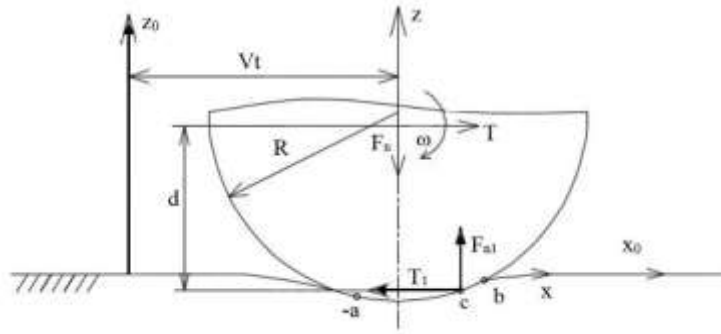


Figure .14. Diagram of contact with sliding and rolling

In the coordinate system (x, y) related to cylinder 1, the relation (49) can be written as

$$, z=0, c < x < b \text{ and } \delta = \frac{\omega R - v \frac{dw_2}{dx}}{v} = \delta \quad (50)$$

δ is the pseudo-slip coefficient. Coulomb-Amontons friction law is accepted inside the slip area (-a, c)

$$, \text{ with } p(x) > 0. \tau_{xz} = -\mu \cdot p(x) \text{sgn}(s_x) \quad (51)$$

Where s_x is the difference between the tangential displacement of velocities at the contact points of the cylinder with the plane:

$$.s_x = \frac{\partial w_2}{\partial t} - v + \omega R = v / \delta - \frac{dw_2}{dx} \quad (52)$$

Outside the contact area (-a, b), the viscoelastic plane is not required. The relationships between the stress and deformation in expressions (34). The solutions given by Goryacheva of the expression (34) are accepted [8]. Thus, the contact width $L = a + b$, the parameter $\varepsilon = \frac{(b-a)}{(b+a)}$, is determined by relations (42) and (43), and the parameter defining the separation of the stick area from the slip area (c) is determined from equation (53).

$$\left(1 + \varepsilon - \beta - \frac{2R\delta}{\mu L}\right) \cdot \left[I_0(\alpha\beta\zeta) \cdot K_1(\beta\zeta) + I_1(\alpha\beta\zeta) \cdot K_0(\beta\zeta) + \frac{1}{\zeta} \cdot \left(\frac{1}{\alpha} - 1\right) \cdot I_1(\alpha\beta\zeta) \cdot K_0(\beta\zeta) \right] \quad (53)$$

Where $\beta = \frac{(b-c)}{(b+a)}$, $I_0(x)$, $I_1(x)$ and $K_0(x)$ are modified Bessel functions. Equation (20) is solved numerically for different values of the parameters α , ζ , in the MATCHAD2000 program. Figure 15 exemplifies the dependence of the dimensionless coordinate $c_a = \frac{c}{L}$

as a function of the parameter $\zeta_{oe} = \frac{LE}{2T\varepsilon v}$, for three parameter values $\alpha = \frac{T\varepsilon}{T\sigma}$,

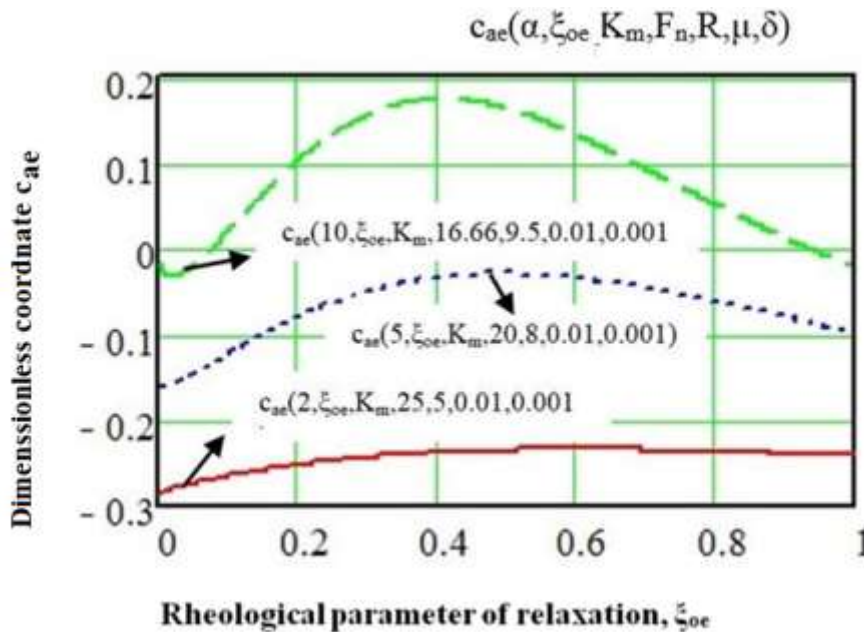


Figure.15. Dependency of the dimensionless cylinder coordinate

It is required by the normal force F_n , the tangential force T and the moment M . As a result of the reactions of the viscoelastic plane appear normal and tangential stresses distributed on the contact area $(-a, b)$, which result in the forces F_{n1} and T . The mechanical equilibrium condition for the cylinder in its center of rotation is

$$M + M_1 + T_1 \cdot R = 0 \tag{54}$$

where $M_1 = \int_{-a}^b x \cdot p(x) dx$ and $T_1 = \int_{-a}^b \tau_{xz} dx$, with $\tau_{xz}(-a) = \tau_{xz}(b) = 0$.

By replacing the pressure $p(x)$ and the coordinates of the points defining the contact (a, b) , Goryacheva deduces:

$$\frac{M_1}{F_n \cdot L} = \frac{\varepsilon}{2} \cdot (1 - L_a^2) + \frac{1}{2\zeta} \cdot \left(L_a^2 - \frac{1}{\alpha} \right) \tag{55}$$

$$\frac{T_1}{\mu \cdot F_n} = 1 - (\beta L_a)^2 - 2\beta L_a^2 \cdot \left(1 + \varepsilon - \beta - \frac{2\delta R}{\mu L} \right) \cdot \frac{K_1(\beta\zeta)}{K_0(\beta\zeta)} \tag{56}$$

The rolling moment of the rigid cylinder on the viscoelastic plane when the normal load F_n , the rolling velocity ω , the axial velocity v is

$$M_{rost} = M_1 + T_1 R \tag{57}$$

Thus, the coefficient of friction by rolling of rigid cylinder of radius R , on a viscoelastic plane characterized by elasticity (E, ν) , creep times (T_ε) and relaxation times (T_σ) and the sliding friction coefficient (μ_r) is given by the relationship

$$\mu_r = \frac{M_{rost}}{F_n \cdot L} = \left(\frac{1}{L_a^2} - 1 \right) \cdot \frac{K_0(\xi)}{4 \cdot K_1(\zeta)} + \frac{1}{2\zeta} \cdot \left(L_a^2 - \frac{1}{\alpha} \right) + \frac{\mu R}{L} \cdot (1 - \beta^2 L_a^2) - \frac{2\mu\beta RL \left(1 - \frac{1}{\alpha} \right) I_1(\alpha\beta\zeta) K_0(\beta\zeta)}{L_a^2 \cdot \zeta \cdot [I_0(\alpha\beta\zeta) K_1(\beta\zeta) + I_1(\alpha\beta\zeta) K_0(\beta\zeta)]} \tag{58}$$

In the case of free rolling $(\mu = 0)$, the expression (58) is reduced to the first two terms. It is exemplified in Figure 16, the dependence of the sliding rolling coefficient for three rigid cylinders $(R = 5; B = 4; R = 8; B = 5; R = 9.5; B = 6 \text{ mm})$ as a function of the parameter

$$\xi_{oe} = \frac{L_0}{2 \cdot T_{\varepsilon \cdot v}}$$

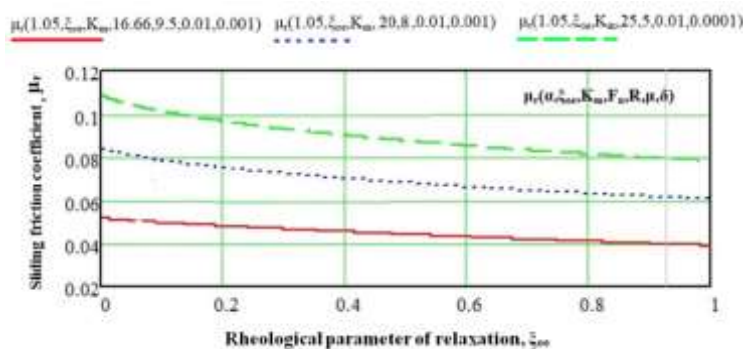


Figure 16 Dependence of the slip coefficient

For pure rolling $(\mu = 0, \delta = 0)$, the variation of the coefficient of friction with the rheological parameter of relaxation of polyethylene (ξ_{oe}) is presented in Figure 17.

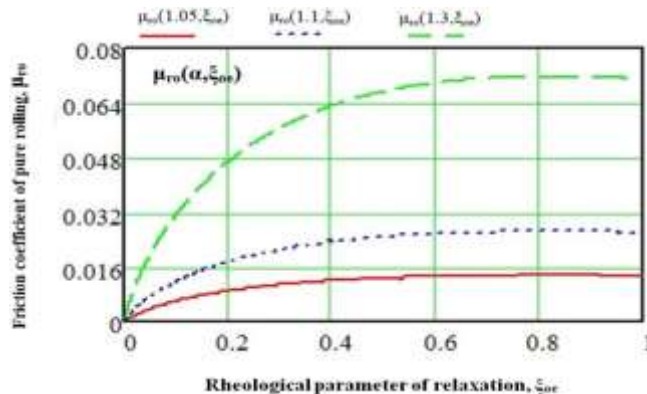


Figure 17 Variation of the coefficient of friction

For the particular case $\alpha = T_\varepsilon / T_\sigma = 1$, the situation of the contact of a rigid cylinder with an elastic plane is obtained. In this situation, the length of contact is

$$L = 2 \cdot a = \sqrt{8 \cdot K \cdot R \cdot F_n} \quad (59)$$

the position of the separating line of stick area from the slip area is

$$\beta = \frac{a-c}{2a} = 1 - \frac{\delta \cdot R}{\mu \cdot a} \quad (60)$$

The pressure distribution is symmetrical

$$(-a < x < a) \cdot p(x) = \frac{\sqrt{a^2 - x^2}}{\pi \cdot K \cdot R}, \quad (61)$$

Tangential stresses in the contact area are

$$\tau_{xz}(x) = \begin{cases} \frac{\mu}{\pi \cdot K \cdot R} \cdot \sqrt{a^2 - x^2}, & (-a < x < c); \\ \frac{\mu}{\pi \cdot K \cdot R} \cdot \sqrt{a^2 - x^2} - \sqrt{(a-x) \cdot (x-c)}, & (c < x < a). \end{cases} \quad (62)$$

The tangential force required to run is

$$\frac{T}{\mu \cdot F_n} = \frac{\delta \cdot R}{\mu \cdot a} \cdot \left(2 - \frac{\delta \cdot R}{\mu \cdot a} \right). \quad (4.63)$$

When a rigid cylinder slides and rolls on a viscoelastic plane, the friction force has a mechanical component due to the asymmetric deformation of the pressure distribution and an adhesion (adhesion) component in the contact area. For the analytical determination of the deformation component of the coefficient of friction of the cylinder on a polyethylene support, the solutions given by Goryacheva [8] and Johnson [6] are proposed.

In this sense, it is accepted that the friction is very small in the contact area ($\mu \approx 0$) and due to the asymmetry of the pressure distribution ($p(x)$) (Figure .18), the results F_{n1} and T_d have moment effects of torsion respect to cylinder axis:

$$T_d = \int_{-a}^a p(x) \sin \varphi \, dx \approx \frac{M}{R}, \quad (4.64)$$

when $M = \int_{-a}^b xp(x) \, dx$

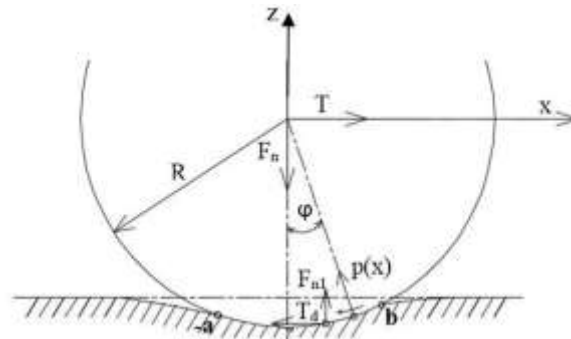


Figure 18 Deformation and force friction components

Since the angle ϕ is small (contact length $l \ll R$) and $\tau_{xz} \approx 0$, it results from (46)

$$\mu_d = \frac{T_d}{F_n} = \frac{M}{F_n \cdot R} = \alpha_h \cdot \frac{L_0}{R}, \quad (65)$$

where α_h is the coefficient of hysteresis losses of viscoelastic polyethylene

$$\alpha_h = \frac{\varepsilon}{2} \cdot L_a \cdot (1 - L_a^2) + \frac{L_a^2 - 1}{2 \cdot \xi_{oe}} \quad (66)$$

With $L_a = \frac{L}{L_0}$, the relative contact width of the viscoelastic cylinder in comparison with an elastic one, $\alpha = \frac{T_\varepsilon}{T_\sigma}$, rheological parameter (relaxation, creep), and $\xi_{oe} = \frac{L_0}{2T_\varepsilon v}$ the relaxation parameter. Considering the average Striebeck loading pressure is

$(p_s = \frac{F_{nt}}{2RB}, F_{nt} = \frac{F_{nt}}{B})$, the dimensionless striebeck pressure is $(p_{as} = \frac{p_s}{E})$, E is the longitudinal modulus of elasticity of polyethylene. The analytical expression of the friction deformation component is resulted

$$\mu_d = 4 \cdot \alpha_h \cdot \sqrt{\frac{2 \cdot (1 - \vartheta^2) \cdot p_{as}}{\pi}} \quad (67)$$

Figure 19 exemplifies the variation of friction component with the rheological relaxation parameter (ξ_{oe}) for three relaxation parameters (α).

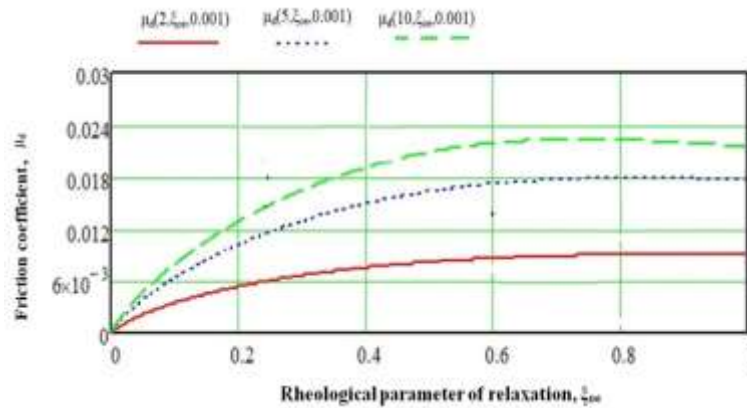


Figure.19 Variation of the friction component with the rheological parameter of relaxation

From the analysis of the deformation component curves of the friction coefficient, it is observed that there are maximum values of certain relaxation modulus (ξ_{oe}) and implicit for certain sliding velocities (v).

5- Conclusions

The rheological behavior of UHMWPE is determined by the spherically connected conical penetrator and the cylindrical penetrator in contact with the UHMWPE plane. The asymmetry of the pressure distribution leads to the formation of a torsional moment in the knee prosthesis. The coefficient of friction by rolling the rigid cylinder on a viscoelastic plane is dependent on the elasticity, the creep and relaxation times. UHMWPE polyethylene can be characterized by the mechanical behavior with a rigid cylinder:

- Contact width for a viscoelastic behavior;
- Pressure distribution and asymmetry on the contact area;
- Coefficient of friction at sliding;
- Coefficient of friction at free rolling;
- deformation component.

6- References

- [1] C. Georgiana, Laurian Tiberiu și Tudor Andrei, „Indentation tests to study the mechanical tribological properties of UHMWPE,” *UPB Scientific Bulletin*, vol. 73, nr. 4, pp. 209-222, 2011.
- [2] B. Georgiana, „Contribuții privind studiul influenței particulelor de uzură asupra durabilității protezelor articulare,” București, 2011.
- [3] J. S. Bergstrom, S. M. Kurtz, Rimnac C.M. și Edidin A.A. , „Constitutive modeling of ultra-high molecular weight polyethylene under large-deformation and cyclic loading conditions,” *Biomaterials*, vol. 23, nr. 11, pp. 2329-2343, 2002.
- [4] J. Bergstrom, C.M. Rimnac și Kurtz S.M, „Prediction of multiaxial mechanical behavior for conventional and highly crosslinked UHMWPE using a hybrid constitutive model,” *Biomaterials*, vol. 24, nr. 8, pp. 1365-1380, 2003.
- [5] J. Valeriu, Physical and thermo-mechanical properties of plastics, Bucharest: Technical Publishing House, 1979.
- [6] K. L. Johnson, Contact mechanics, Cambridge University Press.
- [7] Tudor Andrei, Friction and wear of materials, Bucharest: Bren Publishing House, 2010.
- [8] I. Goryacheva, Contact Mechanics in Tribology, Kluwer Academic, 1998.
- [9] V. L. Popov, Contact Mechanics and Friction, Springer, 2008.